Original Article
Targeting prostate cancer cell proliferation, stemness and metastatic potential using *Costus speciosus* derived phytochemicals

Ayman I Elkady[1,2]

[1]Department of Zoology, Faculty of Science, Alexandria University, Alexandria, Egypt; [2]Department of Biological Sciences, Faculty of Sciences, King Abdulaziz University, Jeddah, Saudi Arabia

Abstract: Prostate cancer is still at the forefront causes of cancer-related morbidity and mortality in men throughout the globe. The disease is initiated and fostered by a subset of cancer stem cells (CSCs). *Costus speciosus* is an oriental herb used in traditional medicine and is a source of bioactive compounds with known pharmacological activities. The present study aims to evaluate the anticancer property of varied extracts isolated from *C. speciosus* against the human prostate cancer PC-3 cells. Extracts derived from *C. speciosus* were analyzed by chromatography-mass spectrometry and their effects on the proliferation, migration, invasion, apoptosis and cell cycle distribution of PC-3 cells were investigated. Results showed that crude hexane extract of *C. speciosus* (CHECS) inhibited proliferation, clonogenic and metastatic potential of PC-3 cells. It induced apoptosis in PC-3 cells associated with generation of reactive oxygen species (ROS), reduction of GSH and permeabilization of mitochondrial and lysosomal membranes, induction of caspase-9/-3 activity and PARP-1 cleavage, DNA damage and an increase in ratio of Bax/Bcl-2 proteins. CHECS induced G_0/G_1 and G_2/M arrest in PC-3 cells and targeted PC-3 prostaspheres. These findings indicate that phytochemicals of CHECS exhibit potential for natural therapeutic product development for prostate cancer.

Keywords: Phytomedicine, apoptosis, metastasis, stem cells, oxidative stress, cell cycle

Introduction

Prostate cancer is the most dominant male malignancy and the second important cause of cancer-related mortality in men throughout the world [1]. It is generally consented that radical prostatectomy, androgen-deprivation therapy and radiotherapy can be remedial for the majority of patients with early-stage prostate cancer, while chemotherapies are always the principal choice for those patients with progressive prostate cancer [2]. However, all these therapies have different side-effects and above all are challenged by the emergence of extrinsic and/or intrinsic resistance in cancer cells [3, 4]. Therefore, there are mounting demands for developing novel agents to overcome these challenges.

Compelling evidences continue to support that prostate cancer is initiated from and constantly replenished by CSCs. This population of CSCs possesses all aspects correlated to tumorigenesis, ranging from tumor initiation, progression, metastases, chemo-/radio-resistance to recurrence [5, 6]. Neither do they secrete androgen receptors [7, 8]; which confer them a marked capability to circumvent androgen deprivation-based treatment strategies. Therefore, in order to eradicate prostate cancer and to prevent recurrence, it is imperative, by no means, to specifically target CSC population [root of tumor] coupled with effective treatments against the larger population of more differentiated tumor cells.

A comprehensive look at the bases of cancerous growths usually reveals an involvement of apoptotic component, which either contributes to disease progression or accounts for it. However, cancer cells develop maneuvers to escape apoptotic cell death in response to physiological stimuli and to cytotoxic agents [6]. This tendency makes most tumors unrespon-

sive to conventional therapies and implies that the induction of apoptosis emerges as a promising strategy for prevention and treatment of cancer. Consistent with this, a plethora of studies indicated that a common denominator of the anticancer drugs, chemopreventive agents, radiotherapies as well as targeted strategies is eradication of tumors via the induction of apoptosis in cancer cells [9]. Apoptotic cell death is activated and tightly regulated by two, but interconnected, signaling pathways, the death receptor-dependent (extrinsic) and the mitochondrial-dependent (intrinsic) pathways [10]. The latter pathway takes over responsibility of prompting apoptotic cell death in response to a wide spectrum of apoptotic stimuli, such as cytotoxic hazards stemmed from chemo-/radio-therapies, oxidative stresses, DNA damage or other unrepairable intracellular insults [10].

For a long time, epidemiological studies as well as preclinical and even early phase-clinical trials have supported the hypothesis that phytochemical compounds derived from oriental herbs can block the initiation or suppress the development various types of malignancies including prostate cancer [11-13]. These phytochemicals gained popularity in recent years being usually multi-targeted and much safer than synthetic drugs [12, 14-16]. Among the innumerable plants that have been researched since ancient time is *Costus speciosus*, a perennial herb native to the south and south east Asian countries. It has long been consumed as an herbal remedy for the treatment a long list of illnesses and a condiment for flavor in cooking. Recently, the herb has attracted an attention as a promising reservoir for supplying bioactive molecules with a wide range of biological activities. For instance, the herb has an applications in pharmaceutical industries as a natural source of diosgenin, a steroidal sapogenin used for synthesis of cortisone, sex hormones and oral contraceptives [17]. In addition, the herb has been found to possess a broad spectrum of pharmacological potentials, including antibacterial, antifungal, antioxidant, antidiabetic, antihyperglycemic, hypolipidemic, antiinflammatory, antistress, antifertility, antipyretic, antidiuretic, hepatoprotective, analgesic and larvicidal activities. Due to too its apparent health benefits, commercial preparations of *C. speciosus* extracts are currently marketed as supplements used for traditional applica-

tions [18, 19]. The rhizomes of the herb are generally consumed in the form of decoction and they possess numerous therapeutic potentials. For example, they have anti-fertility, anabolic and diuretic properties and are prescribed for diseases such as jaundice, urinary diseases, dropsy, rheumatism and pneumonia. Rhizomes have also been found to exhibit CNS depressant activities [20] and to stimulate the uterine contraction due to non-estrogenic effects [21]. An alkaloid extract from rhizomes had papaverine like smooth muscle relaxant and enhances antispasmodic activities [18, 19].

The current study is a part of a large-scale project to seek and develop novel approaches for treatment of prostate cancer using multi-agents of phytochemicals. To attain this aim, the current study was carried out to explore the chemopreventive potential of extracts derived from *C. speciosus* rhizomes on human prostate cancer PC-3 cells and to elucidate the plausible underlying mechanism to provide a lead for development as effective drugs.

Materials and methods

Herbal material and extraction of initial fractionations

500 g air-dried of *C. sepciosus* rhizomes were ground and extracted with 75% methanol for 5 days at ambient temperature. The extract was then, filtered, and concentrated using a rotary evaporator under reduced pressure. The residues were suspended in warm water and further fractionated in a stepwise manner with n-hexane, chloroform, ethyl acetate and n-butanol. The extracts were filtered and rotary evaporated; then the residues of each extract were dissolved in proper volumes of dimethyl sulfoxide [DMSO] to obtain desired concentrations of hexane, chloroform, ethyl acetate and butanol extracts. The DMSO-dissolved extracts were then aliquoted and saved at -20°C until applied to PC-3 cells in cultures.

GC-MS chromatographic conditions

For gas chromatography coupled with mass spectrometry analyses, a Perkin Elmer Clarus 500 GC-MS (Perkin Elmer, Shelton, CT, USA) was utilized throughout the experiments. The

software controller/integrator was TurboMass version 5.4.2.1617. An Elite-1, GC capillary column, Crossbond® 100% dimethyl polysiloxane (30-meter × 0.25 mm ID × 0.25 µm df, Perkin Elmer). The carrier gas was helium [purity 99.9999%] and flow rate was 0.9 mL/min. Source (EI+): source temperature, 230°C. GC line temperature was 210°. Electron energy was 70 eV, and trap-emission was 100 v. The oven was programmed as follows: initial temperature was 100° (hold 4 min) to 210° (rate 5.0°/min, hold 2.0 min), to 270° (rate 10.0°/min, hold 12.0 min), to 280° (rate 10.0°/min, hold 5.0 min) (Run time; 52 min). Injector temperature, 280°. The injection volume was 1.0 µL, and the Split ratio was 1:10. Samples were acquired by applying the total ion chromatogram. The MS scan was from 40 to 400 m/z (500 scan/sec). An average TIC scan of each peak, at definite retention times, was saved using the TurboMass software to characterize the closed peaks obtained from the MS chromatogram of the analyzed samples.

GC-MS sample preparation

One g dried powder of *Costus speciosus* was transferred to 15-mL screw-capped test tube, mixed with 10 mL n-hexane, vortexed for 1 min, left in sonication water bath for 10 min, and left at room temperature for 10 min. The clear supernatant was filtered through 0.22 µ PTFE syringe membrane filter. A volume of 5 mL of this solution was dried with nitrogen gas at room temperature and reconstituted in 1 mL n-hexane. A volume of 1 µL was injected for GC/MS analysis. A total recovery vial 0.9 mL was used. Attached Excel file showed the characterized (confirmed) compounds using NIST2008 program.

Cell lines and cell culture

Human prostate cancer PC-3 cells, breast cancer MCF-7 cells, hepatocellular carcinoma HepG2, colon cancer HCT116 cells and non-malignant human esophageal epithelial cells (OEP) were purchased from King Fahed Biomedical Research Center, King Abdul Aziz University, KSA. Cells were maintained at 37°C in a humidified atmosphere under 5% CO_2 in Dulbecco's modified Eagle's medium (DMEM) containing 10% fetal bovine serum (FBS) and 1% penicillin-streptomycin antibiotics. The cells were subcultured at 2-3 day interval. Exponentially growing cells were seeded at indicated densities in tissue culture plates and treated with displayed concentrations of each extract.

Cell proliferation, clonogenic, anchorage-independent cell growth and scratch wound healing assays

Cell proliferation, clonogenic, anchorage-independent cell growth and scratch wound healing assays were performed as previously detailed [22].

Cell migration and invasion assays

Cell migration and invasion were assessed using Transwell chamber. For the migration assay, PC-3 cells (10^4) were seeded in serum-free DMEM (100 µL) in the top chamber of Transwell inserts (BD Falcon™ 8 µm pore size) and treated with the indicating concentrations of CHECS for 24 h. For the Transwell invasion assay, the cells were seeded in the top chamber of matrigel-coated Transwell inserts (BD Falcon™ 8 µm pore size) and treated with the indicated concentrations of CHECS. The lower chamber was filled with DMEM containing 10% FBS, as a chemo-attractant for 24 h. Then, cells were washed, fixed with 10% formalin-buffered saline for 30 min, stained with 0.5% crystal violet and visualized using a photocamera-equipped light microscope (Leica, Germany).

Culture of PC-3-derived prostaspheres

The PC-3 enriched-tumorspheres (prostaspheres) were isolated, cultured and treated as detailed previously [22]. To assess the inhibitory potential of CHECS on the growth potential of primary sphere-forming cells to serially passage, ($10 × 10^3$/well) were cultured in 96-well ultra-low attachment plate (Corning) for 72 h. The, cells were then treated with the indicated concentrations of CHECS for 72 h, and primary spheres were collected, dissociated, and resuspended in serum-free DMEM/F12 to form secondary spheres. The secondary spheres were cultured for 7 days; after which, cells were dissociated and re-cultured to form tertiary spheres. Images of primary, secondary and tertiary cultures were captured at indicated times using phase contrast microscopy.

Detection of CD44+ and CD133+ cells by flow cytometry assay

Detection of CD44+ and CD133+ positive cells was carried out as following. Briefly, 50 × 10^4 PC-3 cells or PC-3 derived CSCs were incubated with fluorochrome-conjugated monoclonal

antibodies, mouse anti-CD44 antibody (SAB-1405590; Sigma), mouse anti-CD133 (Prominin-1) (MAB4399; EMD Millipore) or isotype control antibody (Mouse IgG1) (Sigma), in the darkness at 4°C for 10 min, then measured by flow cytometry analysis.

Chemoresistance assay

The chemoresistance was assessed using the MTT assay. Briefly, 10^3 cells/well were plated in 96-well plates in 100 µL culture medium for 24 h. Then, cells were incubated with culture medium containing indicated concentrations of cisplatin (Sigma) or control medium for 48 h. Subsequently, MTT assay was carried as mentioned above to assess cell viability.

Toluidine blue staining

To assess the populations of light and dark cells in PC-3 derived prostaspheres and PC-3 adherent monolayer with toluidine blue, the two cell suspensions were stained with toluidine blue staining buffer containing 10 mM HEPES buffer (pH 7.4), 2 mM EDTA, 0.5% bovine serum albumin and 0.4% toluidine blue (Sigma) for 5 min at room temperature. Stained cells were visualized using a photocamera-equipped light microscope (Leica, Germany).

Morphological assays

The morphological characteristics of apoptosis were examined using Giemsa, acridine orange (AO)/ethidium bromide (EtBr) (Sigma) and Hoechst 33342 staining as previously described [22, 23]. Briefly, PC-3 cells were cultured in 24-well culture plates and treated with CHECS for 24 h. The cells were then washed with PBS, labelled with mentioned stains for 30 min at 37°C in the dark and visualized using a photocamera-equipped light microscope (Leica, Germany).

Annexin V-FITC assay for assessment of apoptosis

Briefly, PC-3 cells (300 × 10^3) were cultured in 25 cm^2 culture flasks for 24 h; then cells were incubated with the displayed concentrations of CHECS for 24 h. The cells were then trypsinized, harvested, washed in PBS and apoptosis induced by CHECS was assessed using Annexin V-FITC Apoptosis Detection Kit (Sigma) by flow cytometry as previously described [22].

Measurement of mitochondrial and lysosomal membrane permeabilization

Mitochondrial membrane potential (Δψm) was assessed using Mitochondrial Membrane Potential Assay Kit (Cayman Chemicals), following vendor's recommendations. Briefly, PC-3 cells were cultured in 96-well culture plates and treated with CHECS for 24 h; then, Δψm and fluorescence intensity of the cells were measured as described previously [22].

For lysosomal membrane permeabilization (LMP), PC-3 cells were grown in 96-well culture plates and incubated with CHECS for 24 h. Then, quantitative analyses and fluorescence intensity of the cell cells were measured as described previously [22].

Determination of ROS production

PC-3 cells were grown in 96-well culture plates and incubated with CHECS for 24 h; then ROS level and fluorescence intensity of the cell cells were measured as described previously [22].

Determination of GSH level

PC-3 cells were grown in 96-well culture plates and incubated with CHECS for 24 h as mentioned above. Then, cells were then washed, labelled with 10 µM fluorescent probe, CMFDA (Cayman Chemicals) for 30 min at 37°C in the dark and fluorescence intensity of the cell was measured using a micro-plate reader [BioTek Synergy] with excitation at 492 nm and emission at 517 nm. The cells were also photographed using fluorescence microscope (Leica, Germany).

Single-cell gel electrophoresis (comet assay)

Briefly, PC-3 cells (100 × 10^3 cells/mL) were cultured and treated with CHECS for 24 h as mentioned above. Then, the cells were harvested, resuspended in ice-cold PBS and DNA damage was evaluated by comet assay utilizing OxiSelect™ Comet Assay Kit (Cell Biolabs, Inc) as previously described [22].

DNA fragmentation assay

Briefly, PC-3 cells (100 × 10^3 cells/mL) were cultured and treated with CHECS for 72 h as mentioned above. Then, the cells were harvested, resuspended in ice-cold PBS and DNA was

extracted and gel-electrophoresed as previously described [22].

Cell cycle analysis

Briefly, PC-3 cells (300 × 10³) were cultured and treated with CHECS for 48 h. Then cells were harvested, washed with PBS, fixed in ice-cold 70% overnight ethanol at 4°C and cell cycle analysis was performed essentially as described previously [22].

Western blot analyses

Briefly, PC-3 cells were cultured in six-well plates and incubated with the displayed concentrations of CHECS for 24 h as mentioned above. Next, the cells were harvested, washed in PBS and pelleted by centrifugation. Then, preparation of whole and nuclear protein lysates, polyacrylamide gel electrophoresis, immunoblotting and detection of desired proteins were performed as previously detailed [22].

Statistical analysis

All experiments were performed in triplicate for several times and the results were displayed as mean ± standard deviation (SD). The statistical significance of results was determined by Student's t-test using GraphPad Prism 6 program, and a *p* value of less than 0.05 was considered statistically significant.

Results

Bioassay-guided fractionation of C. speciosus extracts

Initially, the effects of *C. speciosus* extracts on PC-3 cells was determined by analyzing the 24 h dose-response curve to delineate the optimal concentration at which each extract affects growth kinetics of PC-3 cells. The cells were treated with increasing concentrations of methanol, hexane, chloroform, ethyl acetate or butanol extract for 24 h. The growth-inhibitory potentials of all extracts were consistently dose- and time-dependent, monotonic and accumulative, indicating the specific cytotoxic effect of the extracts (**Figure 1A**). The IC$_{50}$ (50% inhibition concentration) values for the extracts were 2.3, 6.0 and 90 µg/mL for hexane, chloroform and methanol, respectively. On the other

hand, the highest doses of ethyl acetate (100 µg/mL) and butanol (500 µg/mL) extracts demonstrated only 45% and 35%, respectively, a reduction in cell viability. These results indicate that hexane extract (CHECS) has the strongest growth-inhibitory potential. So this extract was selected for further analysis and mechanistic studies.
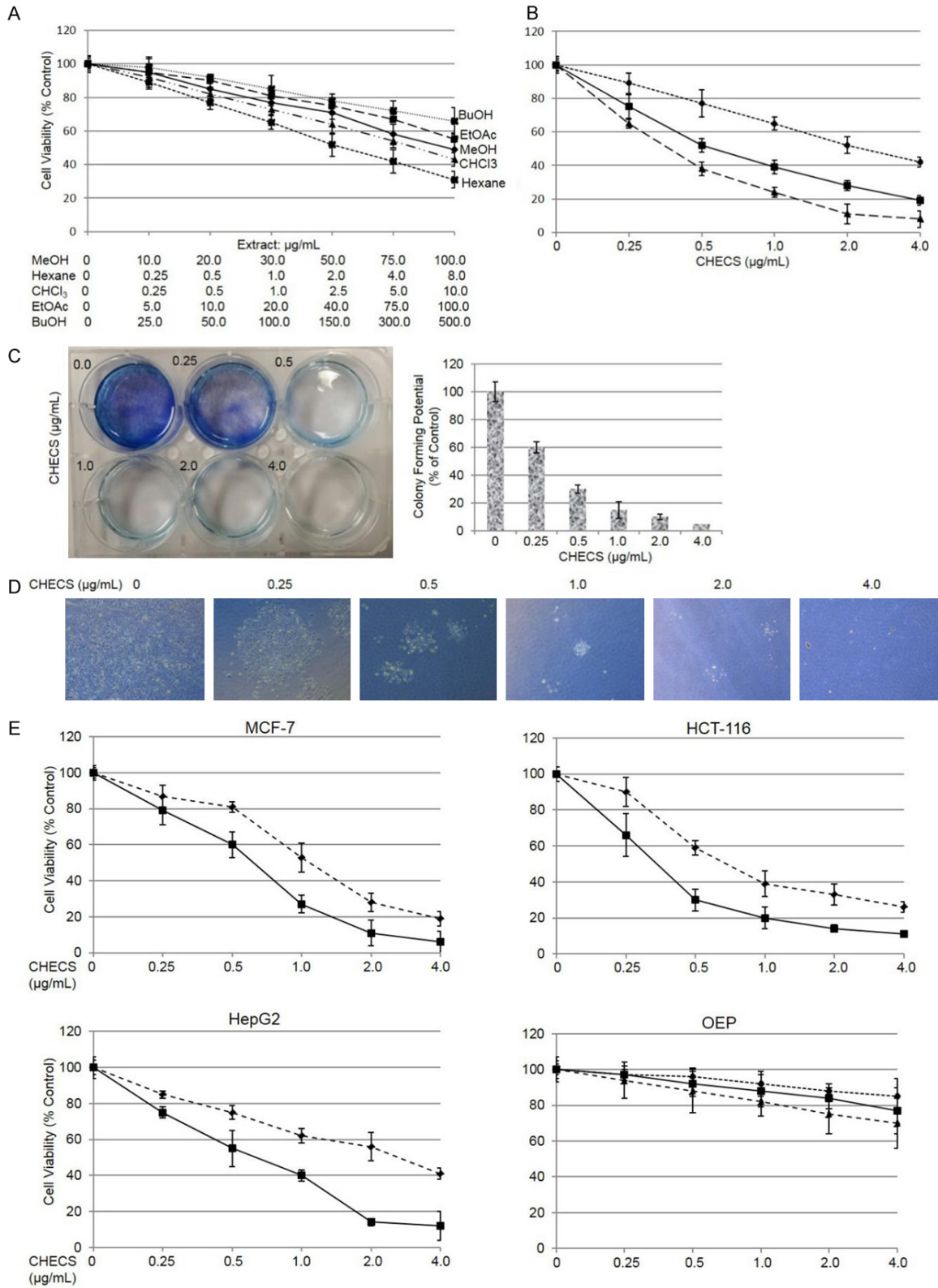
CHECS treatment alters growth kinetics of PC-3 cells

To further characterize the effect of CHECS on growth kinetics of PC-3 cells, the cells were treated with increasing concentrations of CHECS (0.25-4.0 µg/mL) and cell viability was monitored for 24, 48 and 72 h. The response was a dose- and time-dependent, with a 10-60% reduction after 24 h, a 22-75% reduction after 48 h and 35-92% reduction after 72 h (**Figure 1B**). The IC$_{50}$ values at 24, 48 and 72 h were 2.0, 0.5 and 0.35 µg/mL, respectively. All these findings demonstrate that CHECS inhibited the growth of PC-3 cells in a significant manner.

Next, a clonogenic assay was carried out to test whether growth-inhibitory properties of CHECS can affect the clonogenic potential of PC-3 cells. CHECS caused a considerable decrease both in colony number and size compared with control colonies (**Figure 1C**). To validate these results, a soft agar assay was conducted. Once again, a decrease in the number and size of growing colonies were observed following CHECS exposure (**Figure 1D**).

Finally, to validate growth-inhibitory effects of CHECS in the contexts of other cancer cell lines, the time and dose course effects of CHECS on the growth of breast (MCF-7), liver (HepG2) and colon (HCT-116) cancer cell lines were analyzed. As shown in **Figure 1E**, all tested cell lines were especially sensitive to CHECS's growth-inhibitory potential, in a time- and concentration-dependent manner. The IC$_{50}$ for 24 and 48 h treatments appeared to be 1.0 and 0.6 µg/mL for MCF-7, 0.6 and 0.35 µg/mL for HCT-116 and 2.25 and 0.6 µg/mL for HepG2 cells. On the other hand, CHECS exhibited a marginal cytotoxic effect on the non-malignant human esophageal epithelial cells (OEP). The maximal effect was observed after 72 h and at a concentration of 4.0 µg/mL CHECS, where CHECS induced 30% decrease in the percent-

Figure 1. CHECS treatment alters growth kinetics of PC-3 cells. (A) The PC-3 cells were treated with the displayed concentrations of the indicated extracts for 24 h. (B) The PC-3 cells were treated with the indicated concentrations of CHECS for 24 (dotted), 48 (solid) and 72 (dashed) lines. Colony formation (C) and soft agarose (D) assays of PC-3 cells treated with CHECS for 13 days (magnification: 5 ×). The histogram (C) shows the colony forming potential of the cells at each dose of CHECS. (E) The displayed cell lines were treated with the indicated concentrations of the CHECS for 24. Dose points represent mean ± SD of independent experiments in triplicates.
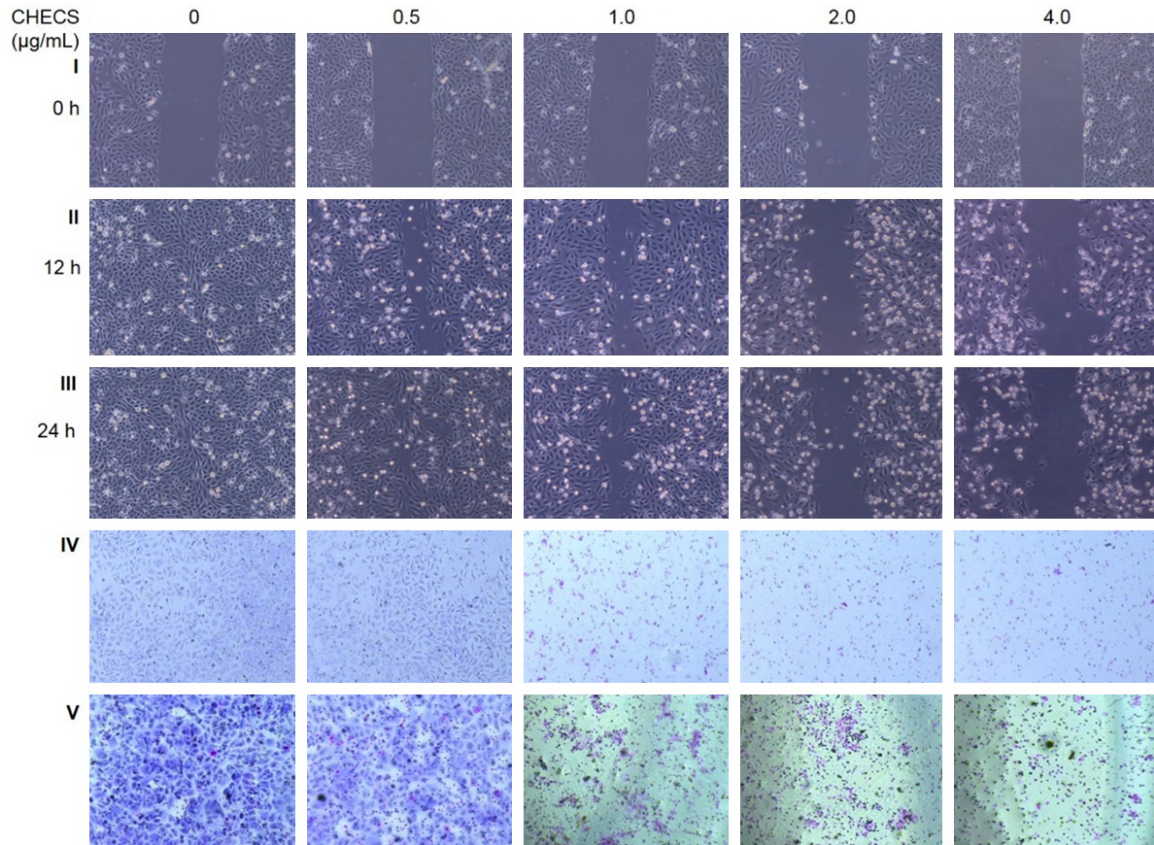
Figure 2. CHECS inhibits invasion and migration of PC-3 cells. Wound healing (Row I, II and III), cell migration (Row IV) and cell invasion (Row V) assays show the inhibitory effect of CHECS on PC-3. In all experiments, images were photographed under a light microscope; magnification of × 20.

age of cell viability (**Figure 1E**). Taken together, these findings denote that CHECS might prevent proliferation or induced apoptosis in cancer cells ultimately resulting suppression of cancer cell growth.

CHECS inhibits invasion and migration of PC-3 cells

Convenient evidences indicated that both cell migration and invasion play a central in the metastasis [6]. To test whether growth-inhibitory properties of CHECS can affects the migration potential of PC-3 cells, the effect of CHECS on PC-3 cell migration was performed using a classic wound healing assay. The results revealed CHECS effectively inhibited the migration potential of treated cells, in a dose- and time-dependent manner (**Figure 2**, Rows I, II and III). The untreated cells replenished the wound area completely after 12 h; in contrast, the cells treated with 0.5 µg/mL CHECS showed a wider wound gap 24 hours and took a longer time to fill in the wound gap. Furthermore, for

the cells treated with the higher concentrations (1.0, 2.0 and 4.0 µg/mL) of CHECS, the wound gaps were not completely filled, indicating a defect in migration. To substantiate these finding the migration assay was repeated using Transwell invasion assay. Consistent with the findings in wound healing assay, CHECS-treated cells exhibited a substantial decrease in the number of migrated cells (**Figure 2**, Row IV). Next, the effect of CHECS on the invasive potential of PC-3 cells was assessed using matrigel-coated Transwell chambers. CHECS decreased PC-3 cell invasion ability in a dose- and time-dependent manner (**Figure 2**, Row V). Collectively, these results imply that CHECS diminished the migratory and invasive potentials of PC-3 cells.

CHECS induces hallmarks of apoptosis in PC-3 cells

To examine whether the cytotoxic of CHECS is linked to the induction of apoptosis, PC-3 cells were treated with increasing concentrations of

CHECS and morphological characteristics of apoptosis were monitored. The images of light microscopy demonstrated that treated cells clearly exhibited significant morphological features of cells committing apoptotic death; these include loss of adhesion, sporadic distribution, shrinkage of cell volume, atypical cell shapes, karyopyknosis and formation of apoptotic bodies (**Figure 3A**, Rows I and II). Next, cells were stained with a mixture of acridine orange (AO) and ethidium bromide (EtBr) and analyzed under fluorescent microscopy. The cells in control culture exhibit homogenous green color indicating cells are viable (**Figure 3A**, Raw III). On the other hand, the CHECS-treated cells exhibited a gradual decrease in green fluorescence accompanied by a parallel increase in red fluorescence. These observations indicate that treated cell lost their membrane integrity, which is a hallmark of cells advancing apoptotic death. Finally, when the cells were stained with a nuclear stain, Hoechst 33342 dye; the nuclei appeared highly bright indicating that CHECS dose-dependently increased the content of chromatin condensation (**Figure 3A**, Row IV), a characteristic signs of apoptotic cell death.

To further confirm the pro-apoptotic potential of CHECS, the percentage of apoptotic cells were analyzed by flow cytometer. The results of these experiments explained that 24 h exposure to CHECS induced an increase in apoptotic cell populations in PC-3 compared to controls (**Figure 3B**). The proportions of cells underwent apoptotic death in right quadrants were increased up to 52.97, 64.7, 87.41 and 92.92% after treating the PC-3 cells with 0.25, 0.5, 1.0, 2.0 and 4.0 µg/mL CHECS, respectively (**Figure 3C**). Taken together all these results are all hallmarks of apoptotic cell death and demonstrate the ability of CHECS to induce apoptosis in PC-3 cells.

CHECS induces accumulation of ROS, depletion of GSH, permeabilization of mitochondrial and lysosomal membranes and activation of caspse-9/-3

To investigate whether ROS generation is involved in CHECS-induced apoptosis, cells were treated with increasing concentrations of CHECS and the level of ROS was quantified using fluorescent probe, DCFH-DA. When cells were incubated with CHECS, the level of ROS increased 2.3-fold above its basal level (**Figure**

4A). Next, the possibility that CHECS-induced production of ROS could deplete intracellular glutathione (GSH) level was investigated using a fluorescent probe, CMFDA. The observations of these experiments indicated that treatment of PC-3 cells with CHECS led to a decline in the means of CMF fluorescent intensity (**Figure 4B**). Collectively, these findings suggest that ROS production is an intermediate step involved in CHECS-induced apoptotic cell death.

Amongst well-known consequences of excessive ROS accumulation is the induction of LMP and MMP [24]. Therefore, the effect of CHECS on the lysosomal integrity was tracked using AO staining; the PC-3 cells were treated with increasing concentrations of CHECS for 24 and labeled with AO. Quantitative analysis show that 4.0 µg/mL CHECS increased the intensity of green fluorescence to 3.5-fold compared to the untreated cells (**Figure 4C**). Compatible with this analysis, fluorescent microscopy images showed that untreated cells obviously displayed red staining of punctuate lysosomes disseminated throughout the cytoplasm indicating the integrity of lysosomal membranes. On the other hand, after CHECS treatments, the cells displayed less intense red fluorescence and more intense green fluorescence, indicating high concentrations of CHECS caused LMP.

To assess whether CHECS-induced ROS accumulation leads to destabilization of the mitochondrial membrane, the collapse of mitochondrial potential, ΔΨm (MMP) was examined after CHECS treatment. The PC-3 cells were treated with increasing concentrations of CHECS for 24 h and were then labeled with the lipophilic dye, JC-1. The spectrophotometric analyses showed that CHECS provoked substantial mitochondrial membrane depolarization, where 4.0 µg/mL CHECS concentration caused ~2.5-fold decrease in the ratio of red/green fluorescence intensity (**Figure 4D**). In addition, fluorescent microscopy observations demonstrated that there is a noticeable dose-dependent disappearance of red fluorescence coupled with increased green fluorescence (**Figure 4D**). Collectively, these findings indicate that CHECS-mediated ROS accumulation and GSH depletion induced MMP and LMP.

Next, the expression levels of the antiapoptotic protein Bcl-2 and the pro-apoptotic protein Bax were analyzed. Western blot analyses showed
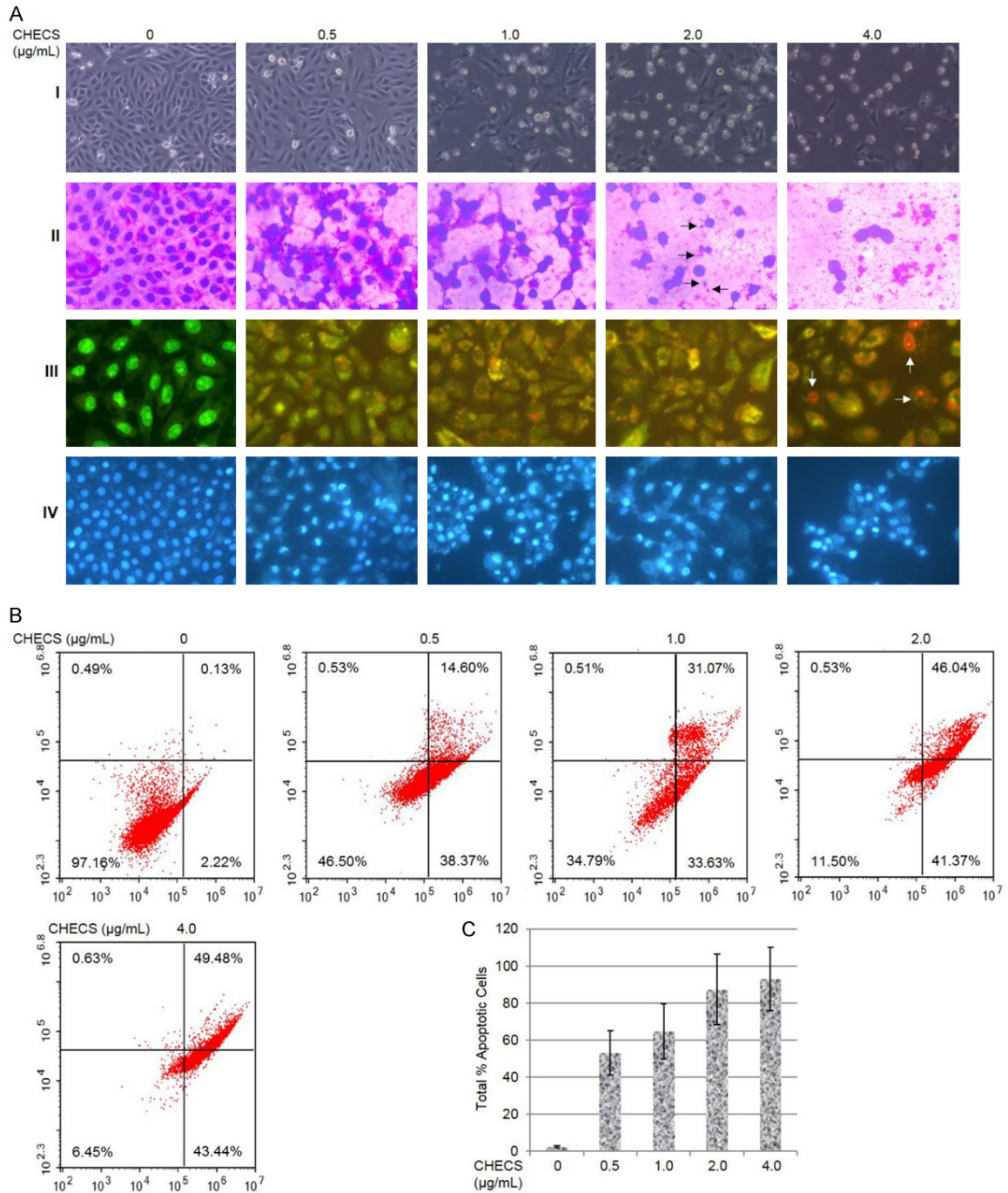
Figure 3. CHECS promotes apoptosis in PC-3 cells. (A) The cells were treated with the displayed concentrations of *CHECS* for 24 h and observed directly under phase contrast microscopy (Row I; magnification: 20 ×), after being labeled with Giemsa stain (Row II; magnification: 20 ×), a mixture of AO and EtBr stains (Row III; magnification: 40 ×) or Hoechst 33342 stain (Row IV; magnification 20 ×). (B) Representative flow cytograms and (C) histogram display total percent of apoptotic cells treated with CHECS; dose points represent mean ± SD of independent experiments in triplicates.

that the treatment of PC-3 cells with CHECS resulted in a marked increase in the expression of Bax and a decrease in the levels of Bcl-2 when compared with control cells. At the level of the highest dose of CHECS (2.0 μg/mL) the

ratio of Bax to Bcl-2 increased 4-fold above its basal level (**Figure 5A**).

To examine the engagement of caspase-9 and -3 activation in apoptotic scenario induced by

2558
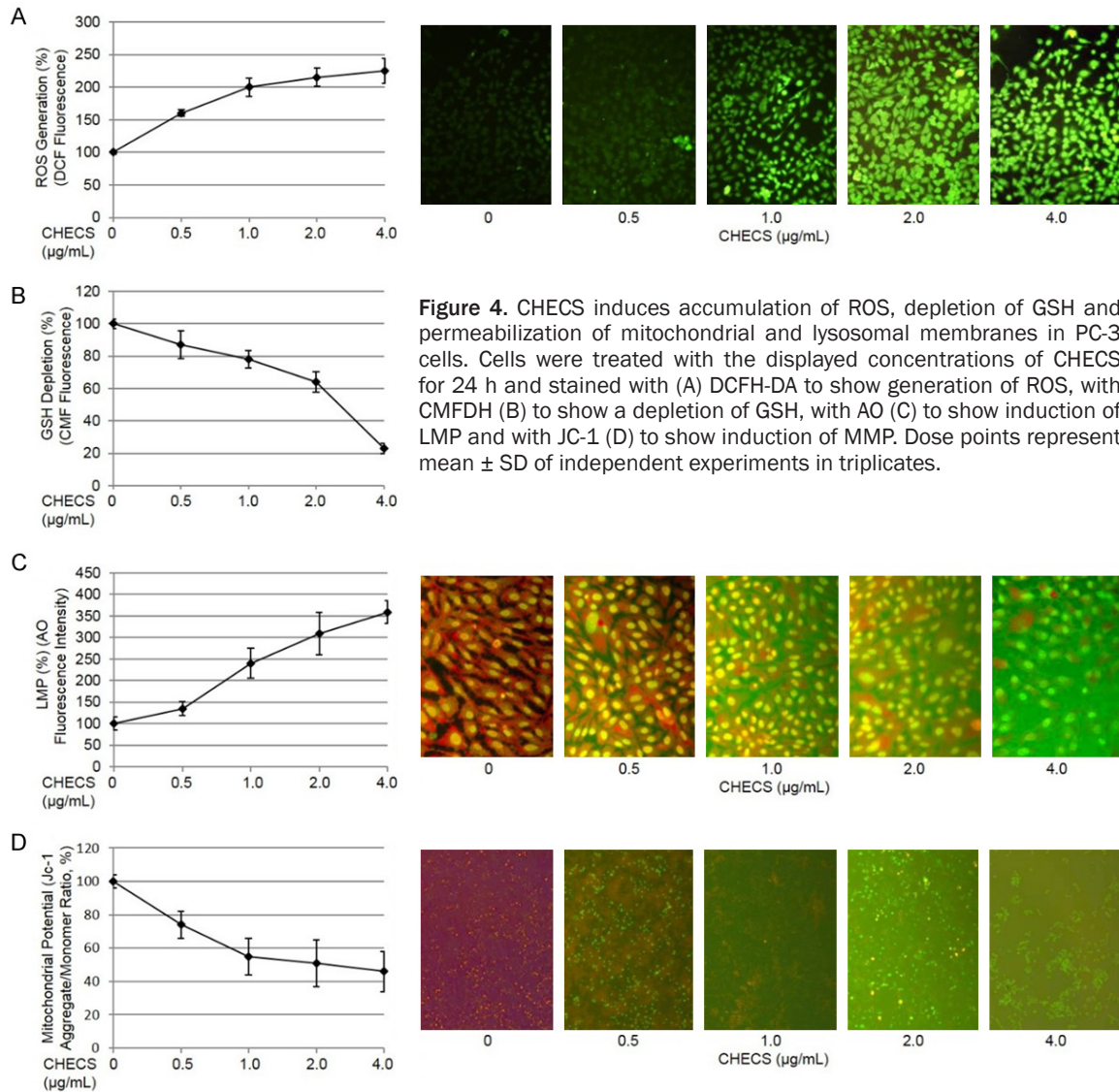
Figure 4. CHECS induces accumulation of ROS, depletion of GSH and permeabilization of mitochondrial and lysosomal membranes in PC-3 cells. Cells were treated with the displayed concentrations of CHECS for 24 h and stained with (A) DCFH-DA to show generation of ROS, with CMFDH (B) to show a depletion of GSH, with AO (C) to show induction of LMP and with JC-1 (D) to show induction of MMP. Dose points represent mean ± SD of independent experiments in triplicates.

CHECS, the activation of both caspases was monitored by flow cytometry. The findings in **Figure 5B** and **5C** clearly indicate that caspase-9 (B) and caspase-3 (C) were markedly stimulated after CHECS treatment in PC-3 cells. Following treatment with 2.0 µg/mL CHECS, there was an increase in the levels of active forms of caspase-9 and caspase-3 by 6.5- and 4.5-fold, respectively. To attain further evidence of caspase-3 activation, the cleavage of PARP-1, a downstream effector of activated caspase-3, was inspected. The flow cytometry analyses confirmed CHECS treatment led to an increase in the level of cleaved PARP-1 (**Figure 5D**). All these findings indicate that CHECS treatment triggered apoptotic cascades in PC-3 cells.

CHECS induces DNA damage and G_0/G_1 and G_2/M phase arrest in the PC-3 cells

To confirm CFENS induces DNA damage leading to apoptotic death, PC-3 cells were exposed to 1.0 µg/mL CHECS and the effect of CFENS on cellular DNA damage was detected, after 24 h, using comet assay. The observations showed the nucleoids of control cells appeared uniformly spherical in shape indicating DNA materials are intact; on the other hand, the nucleoids of CHECS-treated cells emerged as comets indicating a massive DNA damage (**Figure 5E**).

Next, the effect of CHECS on oligo-nucleosomal DNA fragmentation was examined using an
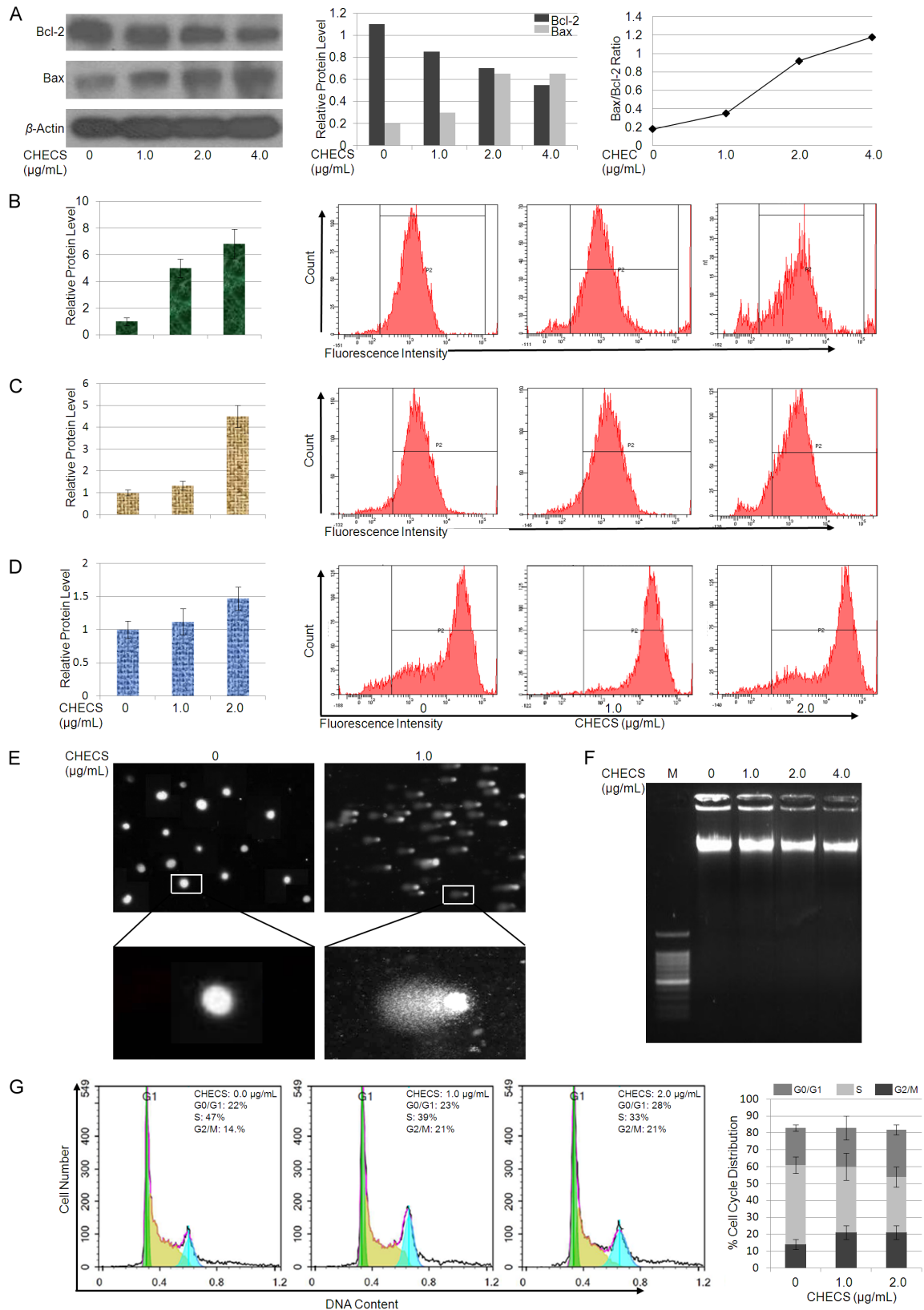
Figure 5. CHECS modulates expression levels of apoptosis-related proteins and induces DNA damage and cell-cycle phase arrest in the PC-3 cells. The PC-3 cells were incubated with the displayed concentrations of CHECS for 24 h and assayed. (A) Expression levels of Bcl-2 and Bax proteins were altered by CHECS treatment as determined by

Western blotting (Left) and quantitative analyses (Right). (B-D) The histograms and representative flow cytograms show CHECS treatment increased activity of caspase-9 (B) and caspase-3 (C) and cleavage of PARP-1 (D). (E) Damage of the genomic DNA after treatment with CHECS as determined by comet assay. (F) CHECS treatments did not induce oligonucleosomal degradation of the genomic DNA after treatment for 72 h. (G) Cell-cycle progression was arrested at the G_0/G_1 and G_2/M phases after treatment with CHECS for 48 h. Dose points represent mean ± SD of independent experiments in triplicates.

agarose gel electrophoresis. The PC-3 cells were treated with increasing concentrations of CHECS for 24, 48 and 72 h; then DNA fragmentation was analyzed. As shown in **Figure 5F**, no DNA fragmentation was observed even after as high as 4.0 µg/mL of CFENS for 72 h treatment. These findings suggest that CFFNS employs non-classical DNA fragmentation scenario to process chromatin during apoptosis.

To investigate the effect of CHECS on cell cycle progression, the PC-3 cells were treated with increasing concentrations of CHECS for 48 h and the cell cycle phases were monitored by flow cytometry. At a level of 1.0 µg/mL, CHECS induced increase in G_2/M phase from 14% to 21%, which was associated with a decrease in S phase from 47% to 39% suggesting that CHECS may have caused cells to accumulate in G_2/M. Upon increasing concentration of CHECS to 2.0 µg/mL, there was an increase in G_0/G_1 from 23% to 28%, which was associated with a parallel decrease in S phase from 39% to 33% hinting that CHECS arrested cells at G_0/G_1 phase (**Figure 5G**). These findings suggest that CHECS significantly halt cell proliferation via hampering progression of the cell cycle at the G_0/G_1 and G_2/M phases.

CHECS inhibits the growth of PC-3-derived CSCs

To explore whether CHECS could inhibit the growth of prostate CSCs, PC-3 derived tumorspheres were isolated, from the cultured PC-3 cells using tumorsphere formation assay. Microscopic observations revealed some cells formed clonal non-adherent prostaspheres and could also be serially passaged signifying that they possess CSC properties (**Figure 6A**). Thereby, it is reasonable to assume that the PC-3 cell-derived prostaspheres contain stem-like cells.

Next, the cultured prostaspheres were analyzed to assess the existence of hypothesized CSC-like properties; the expression levels of the distinct prostate CSC markers, CD133+ and CD44+ [5, 25], were analyzed. Flow cytometric
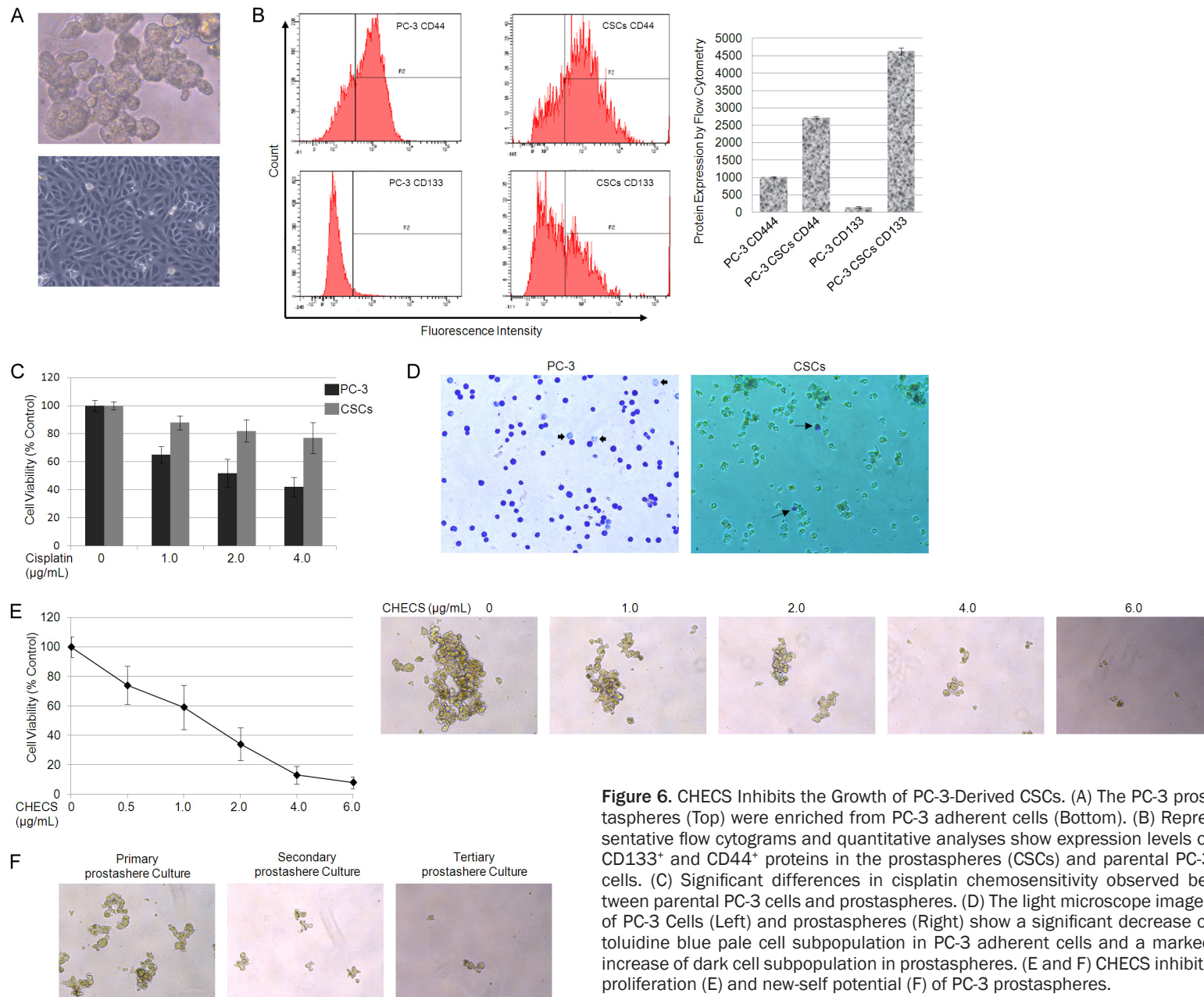
analyses indicated that PC-3 prostaspheres expressed obviously elevated protein levels of CD133+ and CD44+ markers than the parental counterparts (**Figure 6B**). There were a 32-fold increase in CD133+ expression and a 2.7-fold increase in CD44+ expression in spheres compared with adherent PC-3 cells.

To evaluate the chemoresistance properties of the PC-3 prostaspheres and a parental adherent PC-3 cells, the two cell populations were exposed to cisplatin for 48 h and their sensitivities to the drug were compared. The observations of these experiments showed viability of PC-3 prostaspheres was generally higher than adherent PC-3 cells at the alike doses of the drug (**Figure 6C**). At the level of 1.0, 2.0 and 4.0 µg/mL cisplatin, the survival rates of PC-3 prostaspheres were 1, 3-, 1.6-, 1.8-folds, respectively, higher than survival rates of parental PC-3 cells.
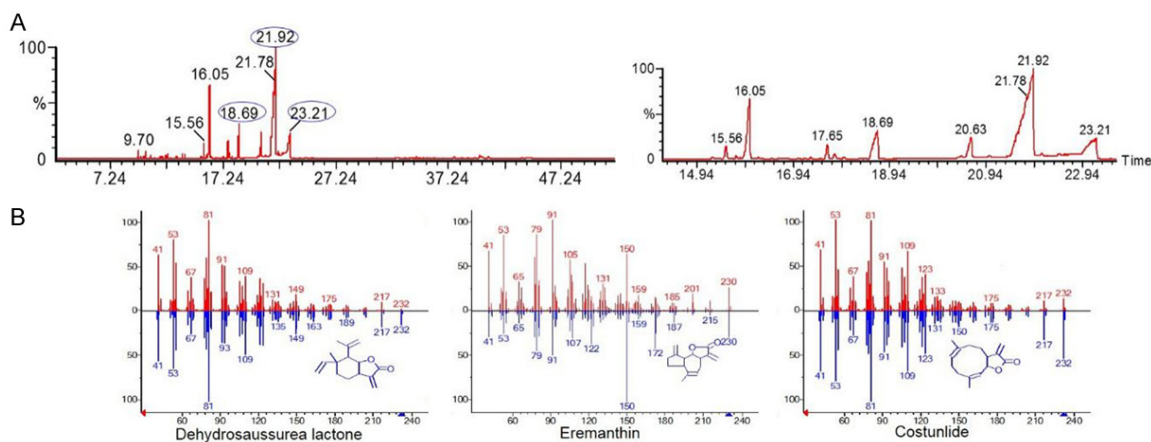
Next, both PC-3 prostaspheres and parental PC-3 cells were stained with toluidine blue and visualized. The findings of this stain indicated that there was a marked decrease of toluidine blue pale cell subpopulation and the increase of dark cell subpopulation in adherent PC-3 cells compared with PC-3 prostaspheres (**Figure 6D**). Taken together, these assays demonstrate that PC-3 derived tumorspheres possess the putative characteristics of cancer stem cells.

To determine whether CHECS would be able to overcome acquired chemotherapy resistance of PC-3 prostaspheres, the prostaspheres were treated with escalating concentrations of CHECS for 72 h and the percentages of growth inhibition were determined. The observations of these experiments demonstrate that CHECS treatments dose-dependently inhibited the growth of PC-3 prostaspheres with an IC_{50} value of 1.25 µg/mL; meanwhile a dose of 6.0 µg/mL CHECS caused a 95% decrease in prostasphere growth (**Figure 6E**). These data imply that the PC-3 prostaspheres are responsive to the cytotoxic effect of CHECS.

Figure 6. CHECS Inhibits the Growth of PC-3-Derived CSCs. (A) The PC-3 prostaspheres (Top) were enriched from PC-3 adherent cells (Bottom). (B) Representative flow cytograms and quantitative analyses show expression levels of CD133+ and CD44+ proteins in the prostaspheres (CSCs) and parental PC-3 cells. (C) Significant differences in cisplatin chemosensitivity observed between parental PC-3 cells and prostaspheres. (D) The light microscope images of PC-3 Cells (Left) and prostaspheres (Right) show a significant decrease of toluidine blue pale cell subpopulation in PC-3 adherent cells and a marked increase of dark cell subpopulation in prostaspheres. (E and F) CHECS inhibits proliferation (E) and new-self potential (F) of PC-3 prostaspheres.

Figure 7. Chemical Identification of CHECS. A. Base peak chromatograms of *C. speciosus* hexane fraction recorded in GC-MS. B. Mass spectra of some major identified peaks. Red (Top Panels) analyses are identified peaks and blue (Bottom Panels) analyses represent identical compounds found in synthetic compound libraries; dehydrosaussurea lactone, 9.1%; RT 18.69; eremanthin, 61.3%; RT 21.92 and costunlide, 3.27%; RT 23.21.

To confirm that CHECS can inhibit self-renewal potential of PC-3 prostaspheres, the clonal expansion (formation of secondary and tertiary spheres) of the prostaspheres was monitored after including CHECS in the medium during primary prostaspheres formation. The prostaspheres were seeded and treated with 1.0 µg/mL CHECS for 72 h to evaluate the potential of a secondary spheroid formation. Then, the cells were dissociated and reseeded at low density to allow self-renewing for two weeks. As clearly seen in **Figure 6F** when CHECS was added to the culture media of the primary prostaspheres, it inhibited the ability of cells isolated from these spheres to form secondary prostaspheres by more than 50% and to form tertiary prostaspheres compared to control culture. These findings denote that CHECS affect prostate stem cell self-renewing potential and that this process is irreversible since the removal of CHECS did not restore the ability of these cells to form prostaspheres upon serial passage.

Chemical identification of CHECS

The total ion chromatogram profile is displayed in **Figure 7**: To identify the most active ingredients in CHCES, the extract was analyzed by GC-MS. The total ion chromatogram profile indicated that CHECS contained three dominant peaks, constituting 73.67% of the UV detectable components of the total mixture (**Figure 7A** and **7B**; original materials will be supplied upon request). The largest peak was eremanthin, detected at 21.92 min and constituted

61.3% of the extract. Eremanthin is followed by dehydrosaussurea lactone (9.1%) and costumlide (3.27%); they were detected at 18.69 and 23.21 min, respectively. Some of the other minor peaks, recorded in data base and others not recorded and identification of these constituents is in progress.

Discussion

Comprehensive studies in *in vitro* and *in vivo* approaches as well as human epidemiological trials demonstrated dietary derived phytochemicals could offer preventive and therapeutic competences against different types of cancers, including prostate phenotype [11-13]. In this study, the cytotoxic effect of methanol, hexane, chloroform, ethyl acetate and butanol extracts derived from *C. speciosus* were individually tested on PC-3 cells. The results herein support the premise that among the five tested extracts, the hexane extract (CHECS) emerges to be the most suitable candidate for restricting the growth of PC-3 cells. This is because its growth-inhibitory potential surpassed all those of the other extracts. It also exerted a marked anti-proliferative activity against the breast, liver and colorectal cancer cell lines and significantly it showed a minimal cytotoxic effect against the growth of normal cell line. The growth-inhibitory properties of CHECS were further backed up by the results from clonogenic and soft agar assays. Findings of these assays are noteworthy since the clonogenic assay assesses the ability of a single cell to prolifer-

ate indefinitely to form a large colony/clone and a reduced clonogenic potential implies a loss of invasion potential in tumor cells [26]. The soft agar assay assesses the potential of a single cell to grow unattached to a substrate; this mode of growth is a hallmark of cell transformation [26, 27] and accounted as an initial stage in carcinogenesis and as a marker for metastatic potentials of cancer cells in vivo. A loss of the ability to grow in soft agar indicates a decrease in metastatic potential of cancer cells [28]. Therefore, inability of PC-3 cells treated with CHECS to form clones or to grow in soft agar compared to control cells adds further evidence demonstrating the anti-carcinogenic potential of CHECS.

It is documented that metastasis is the major causes of morbidity and mortality in cancer patients [29]. The key events in the metastatic process are related to the invasion and migration potentials of cancer cells [6]. The findings herein indicated that CHECS consistently impeded invasion potential of PC-3 cells, diminished healing of the scratched PC-3 monolayers and restrained the migration potential of the PC-3 cells to the bottom chamber in Transwell invasion assay. Thus, all these findings strengthen the potential development of CHECS as an anti-metastatic agent in prostate cancer.

An overwhelming body of evidence accumulated in the last decades indicated that a key property of a candidate anticancer agent is the induction of apoptosis in cancer cells, which discriminates between cytotoxic drugs and toxic compounds [30, 31]. In addition, clinical observations explain that induction of apoptosis prompts complete eradication of established tumors in vivo without causing deleterious effects to normal cells [32]. The light and fluorescent microscopy analyses indicated that the CHECS-treated PC-3 cells exhibited typical morphological features of apoptotic cell death. The observations of the morphological analyses were also corroborated by flow cytometer analysis. The results of this analysis showed that the proportions of cells in the lower- and upper-right quadrants corresponding to early and late apoptosis cells, respectively, increased after treating the PC-3 cells with CHECS. All these findings suggest that CHECS treatment might induced apoptosis in PC-3 cells, which may underlie the reduction of cell viability.

Elucidating the potential molecular mechanisms underlying the induction of apoptosis in PC-3 by CHECS revealed that CHECS provoked events leading to an increase in ROS. These findings deserve attention, since cumulative studies indicated that most phytochemicals exert their pro-apoptotic potential through induction of ROS [33]. The results herein showed that CHECS dose-responsibly increased ROS level and depleted GSH pool in PC-3 cells, implying the cells suffer oxidative stress. Therefore, the pro-apoptotic activity of CHECS was accompanied by the generation of ROS and PC-3 cell death by CHECS is a ROS-dependent process. Despite the details of how CHECS induced oxidative stresses are not yet known and demand further investigations, one possibility, CHECS generated excessive amount of ROS that facilitate the consumption of GSH or CHECS might directly or indirectly reduced regeneration or synthesis of GSH.

Experimental evidences indicated that high levels of ROS can induce LMP and MMP [34]. The incidence of LMP results in the release of lysosomal enzymes to the cytosol, where they digest cellular biomolecules and organelles leading to the execution of apoptotic scenario, through caspase-dependent and -independent pathways [35]. Similarly, induction of MMP leads to the release of apoptogenic factors (such as cytochrome *c*) that initiate the activation series of biochemical reactions resulting in stimulation of caspase-3, an apoptosis-executing caspase [10]. Therefore, the induction of either LMP or MMP is sufficient to trigger downstream cascades of apoptosis. LMP was analyzed after treatments of PC-3 cells with CHECS, using AO vital stain. The fluorescent microscopy observations showed that untreated cells displayed distinct red fluorescence indicating lysosomes are intact. In contrast, in treated cells, red fluorescence was reduced and green fluorescence was maximally increased, nearly 3.5-fold above its basal level indicating that LMP is involved in CHECS-induced cell apoptosis.

MMP was also analyzed after treatments of PC-3 cells with CHECS, using JC-1 dye. The fluorescent microscopy observations demonstrated that untreated cells fluoresce red indicating presence of electrochemical potential across the mitochondrial membrane. On the other hand, upon exposure to CHECS, the intensity of

red fluorescence dimmed gradually, whilst the intensity of green became the maximal indicating release of JC-1 dye molecules into cytosol due to loss of mitochondrial membrane potential. Quantitative analysis showed that the cells exposed to CHECS exhibited dose-dependently a decrease in JC-1 aggregate/monomer ratio, where the red/green fluorescent ratio decreased down to 40% of its basal level in untreated cells. Thereby, these findings imply that LMP and MMP could be, at least in part, a key factor involved in CHECS-induced apoptosis. LMP- and MMP-mediating apoptosis induction is not unique to CHECS and was indicated in a long list of phytochemicals-derived chemopreventive agents and nutritional supplements [36-38].

At the molecular level, both Bcl-2 and Bax proteins are the most important players controlling the permeability of mitochondrial membrane [10]. The expression ratio of Bax to Bcl-2, rather than individual expression of each protein, determines the susceptibility of a cell to commit suicide or to maintain survive [39] and is considered a prognostic marker for therapeutic response to radiotherapy [40]. The Western blot analysis clearly showed treatment of PC-3 cells with CHECS led to a dose-dependent increase in the level of Bax with a parallel decrease in Bcl-2 levels, resulting in an increase in the ratio of Bax/Bcl-2 protein levels, thereby, tipping the balance of cell survival/apoptosis toward the latter.

Consistent with the increase of Bax/Bcl-2 ratio are the findings of flow cytometer showing activation of caspase-9, caspase-3 and cleavage of PARP-1. The caspase-3 works at the most distal stage of the apoptotic cascade and upon its activation, it mediates the cleavage and inactivation of key cellular proteins such as PARP-1, a central player involved in DNA repair [41]. Herein, the flow cytometer analysis demonstrated an increase in the level of cleaved PARP-1. In addition, the observations of comet assay (generally accepted as an indicator of apoptosis [42]) showed that the DNA in PC-3 cells treated with CHECS exhibited typical comet head and fan-like shape tail, implying most DNA migrated out nuclear compartment due to a massive DNA damage and breakdown of nuclear scaffold. Since when cells suffer severe DNA damage, they activate apoptotic signaling [43] and many chemopreventive

agents have been found to impart their apoptogenic potential through induction of DNA damage in cancer cells [44], thereby, it is rational to conclude that CHECS caused severe DNA damage in PC-3 prompting apoptotic signaling.

The observations of cell cycle analysis herein explain that induction of cell cycle arrest seems to be the mechanism underlying inhibition of PC-3 proliferation following CHECS treatment. At a level of 1.0 µg/mL CHECS treatment, the population of PC-3 cells at G_2/M phase was increased at the expense of S phase cell population. Furthermore, increasing concentration of CHECS up to 2.0 µg/mL led to the accumulation of PC-3 cells in G_0/G_1 phase, which was associated with a further decrease in S phase cell population indicating that CHECS can modulate cell cycle phases based on the exposure dose. Most chenopreventive agents induce G_0/G_1 or G_1/M phase arrest and some can agents induce arrest in both phases [45]. Herein, the results show that CHECS induced cycle arrest at G_0/G_1 and G_2/M phases. An explanation for this dual arrest is the mixture formula of the CHECS, which comprises different classes of ingredients. These ingredients have substantially different biochemical properties and mostly target different molecular targets in cell cycle machinery resulting in cycle arrest in both phases. Further investigations are on progress to decipher the molecular targets of CHECS in each phase of the cell cycle. Similar to CHECS, berberine-induced G_0/G_1 and G_2/M phase arrest in PC-3 [46]. The results herein explain that DNA damage detected by comet assay was observed 24 h post CHECS treatment, whilst cell cycle arrest was noticed 48 h post-CHECS exposure. Thus, the timeframe required to induce DNA damage was shorter than that needed to provoke PC-3 cell cycle arrest, suggesting that DNA damage might be an upstream event leading to cell cycle arrest.

Clinical evidences indicated prostate CSCs foster progression of the tumor and pose formidable challenges to attain curative therapies in patients [5, 25]. In this study, the impact of CHECS's growth inhibitory properties on the viability of CSCs derived from PC-3 tumorspheres was investigated. Initially, isolated spheres were characterized to confirm they possess the putative prostate CSC properties. The gold standards for evaluating the presence of CSCs involve the ability to form spheres and

to express the positive stemness markers [47, 48]. The results herein demonstrate the prostaspheres could be serially passaged forming further tumorspheres indicating that these cells possess CSC properties. In addition, flow cytometry analysis indicated the expression levels of CD133^{+} and CD44^{+}, representative stem cell surface markers of PC-3 [49], were higher in the growing prostaspheres than in parental PC-3 cells indicating these prostaspheres possess prostate CSCs. The identification of CD44^{+} expression in the prostaspheres indicates the authenticity of CSC properties since it is a basal cell marker characteristic to human prostate CSCs and prostate cancer cell lines sorted for high expression of CD44^{+} exhibited enhanced expression of other stemness markers [5, 50]. Furthermore, studies on human prostate cancer cell lines and xenografts demonstrated the CD44^{+} population is more proliferative, clonogenic, tumorigenic, and metastatic than CD44^{-} cells. Finally, CD44^{+} + CD133^{+} subpopulations obtained from human tissue have enhanced capacity for in vitro serial passaging [51-53]. Herein, the PC-3 derived prostaspheres were also more resistant than parent adherent monolayer PC-3 cells to the cytotoxic effect of cisplatin and exhibited the minimal appearance of cells stained with toluidine blue. All these observations indicate that the PC-3 derived tumorspheres cultured in this study exhibited stemness properties. Mounting evidences confirmed assessing the in vitro anti-self-renewal potential of phytochemicals and herbal extracts by tumorsphere assay could reflect the anti-tumorigenic potential of those agents in vivo [54, 55]. One of the seminal findings in the present study explains that when CHECS was included in the medium of prostasphere cultures, the cells underwent apoptotic death indicating that CHECS possesses a potential to overcome acquired chemotherapy resistance and to inhibit the growth of CSCs. Furthermore, when CHECS was included at an early stage of culture, during primary prostasphere formation, it significantly reduced the clonal expansion of the prostaspheres; they were barely able to form secondary prostaspheres and failed completely to form tertiary prostaspheres. Therefore, on the top of its ability to kill highly proliferating PC-3 cells, CHECS did inhibit growth of PC-3 derived CSCs. Thus, these findings suggest the therapeutic benefit of the CHECS is in its ability to inhibit the PC-3 proliferating cells and to target the resistant CSCs pool, making it to be a suitable candidate for restricting the growth of PC-3 cells and for potential development as a chemopreventive regimen for prostate cancer.

The *C. specious* rhizome is a source of a number of bioactive compounds; albeit some of which were compiled, the full range of the compounds has not yet been identified [56]. Herein, the ingredients in *C. specious* rhizomes were successively extracted with methanol, hexane, chloroform, ethyl acetate and butanol, and the bioassay-guided fractionation analysis indicated the anti-proliferative potentials of the extracts gradually decreased in the following rank order: hexane > chloroform > methanol > ethyl acetate > butanol. Thus, the most potent chemopreventive ingredients in the rhizomes reside in hexane. To attribute the observed growth-inhibitory potential of hexane extract to definite component[s], GC-MS analysis was pursued. The analysis identified some major compounds with well-known pharmacological potentials as well as many others with unknown and/or untested activity. The most well-known ingredient identified in the extract was costunolide, a common secondary metabolite found in important medicinal plants and previously isolated from the hexane extract of *C. speciosus* [57]. The existence of costunolide in CHECS may elucidate the observed cytotoxic properties of the CHECS, since it exhibited marked anti-cancer activities against various cancer cell lines including prostate cancer [58-60] and inhibited growth of colon cancer in vivo [61]. In addition, costunolide and eremanthin, another constituent found in CHECS, exhibited marked antioxidant activity in vivo, which is a hallmark of chemopreventive agents [62]. Therefore, it seems that the cytotoxic potential of CHECS might be imparted by additive and/or synergistic interactions of its individual constituents.

In conclusion, the current study demonstrate CHECS inhibited the proliferation, clonal growth, invasion and migration of PC-3 cells via induction of apoptosis. The apoptotic death was associated with accumulation of ROS, depletion of GSH, induction of LMP and MMP, DNA damage and cell cycle arrest. CHECS also down-regulated expression of Bcl-2, upregulated expression of Bax and stimulated activation of caspase-3 and cleavage of PARP-1. Additionally, CHECS was able to target the growth of PC-3 enriched in tumorsphere cultures. The

results herein put forth essential information on the action of CHECS for justification as a potential source of anticancer drug leads. The forthcoming challenge will be to determine the effect of CHECS on critical genes associated with prostate cancer and to evaluate the efficacy of CHECS on xenograft models of prostate cancer. Studies are conducted to identify untested active constituents and an effective combination among CHECS individual constituents for their optimal utilization.

Acknowledgements

Disclosure of conflict of interest

None.

Address correspondence to: Ayman I Elkady, Department of Zoology, Faculty of Science, Alexandria University, Alexandria, Egypt; Department of Biological Sciences, Faculty of Sciences, King Abdulaziz University, Jeddah, Saudi Arabia. Tel: +966-530-676470; Fax: +966-2-6952290; E-mail: aielkad@yahoo.co.uk; aealkadi@kau.edu.sa

References

[1]   Siegel RL, Miller KD, Jemal A. Cancer statistics, 2017. CA Cancer J Clin 2017; 67: 7-30.

[2]   Cornford P, Bellmunt J, Bolla M, Briers E, De Santis M, Gross T, Henry AM, Joniau S, Lam TB, Mason MD, van der Poel HG, van der Kwast TH, Rouvière O, Wiegel T, Mottet N. EAU-ESTRO-SIOG guidelines on prostate cancer. Part II: treatment of relapsing, metastatic, and castration-resistant prostate cancer. Eur Urol 2017; 71: 630-642.

[3]   Tran C, Ouk S, Clegg NJ, Chen Y, Watson PA, Arora V, Wongvipat J, Smith-Jones PM, Yoo D, Kwon A, Wasielewska T, Welsbie D, Chen CD, Higano CS, Beer TM, Hung DT, Scher HI, Jung ME, Sawyers CL. Development of a second-generation antiandrogen for treatment of advanced prostate cancer. Science 2009; 324: 787-90.

[4]   Beer TM, Armstrong AJ, Rathkopf DE, Loriot Y, Sternberg CN, Higano CS, Iversen P, Bhattacharya S, Carles J, Chowdhury S, Davis ID, de Bono JS, Evans CP, Fizazi K, Joshua AM, Kim CS, Kimura G, Mainwaring P, Mansbach H,

Miller K, Noonberg SB, Perabo F, Phung D, Saad F, Scher HI, Taplin ME, Venner PM, Tombal B; PREVAIL Investigators. Enzalutamide in metastatic prostate cancer before chemotherapy. N Engl J Med 2014; 371: 424-33.

[5]   Collins AT, Berry PA, Hyde C, Stower MJ, Maitland NJ. Prospective identification of tumorigenic prostate cancer stem cells. Cancer Res 2005; 65: 10946-51.

[6]   Hanahan D, Weinberg RA. Hallmarks of cancer: the next generation. Cell 2011; 144: 646-74.

[7]   Rybak AP, Bristow RG, Kapoor A. Prostate cancer stem cells: deciphering the origins and pathways involved in prostate tumorigenesis and aggression. Oncotarget 2015; 6: 1900-19.

[8]   Zhang K, Zhou S, Wang L, Wang J, Zou Q, Zhao W, Fu Q, Fang X. Current stem cell biomarkers and their functional mechanisms in prostate cancer. Int J Mol Sci 2016; 17.

[9]   Call JA, Eckhardt SG, Camidge DR. Targeted manipulation of apoptosis in cancer treatment. Lancet Oncol 2008; 9: 1002-11.

[10]   Wong RS. Apoptosis in cancer: from pathogenesis to treatment. J Exp Clinl Cancer Res 2011; 30: 87.

[11]   Lu J, Kim SH, Jiang C, Lee H, Guo J. Oriental herbs as a source of novel anti-androgen and prostate cancer chemopreventive agents. Acta Pharmacol Sin 2007; 28: 1365-72.

[12]   Nirmala MJ, Samundeeswari A, Deepa PS. Natural plant resources in anti-cancer therapy-A review. Research in Plant Biology 2011; 1: 01-14.

[13]   Bommareddy A, Eggleston W, Prelewicz S, Antal A, Witczak Z, McCune DF, Vanwert AL. Chemoprevention of prostate cancer by major dietary phytochemicals. Anticancer Res 2013; 33: 4163-74.

[14]   Liu RH. Potential synergy of phytochemicals in cancer prevention: mechanism of action. J Nutr 2004; 134 Suppl: 3479S-3485S.

[15]   Qurishi Y, Hamid A, Majeed R, Hussain A, Qazi AK, Ahmed M, Zargar MA, Singh SK, Saxena AK. Interaction of natural products with cell survival and signaling pathways in the biochemical elucidation of drug targets in cancer. Future Oncol 2011; 7: 1007-1021.

[16]   Safarzadeh E, Sandoghchian Shotorbani S, Baradaran B. Herbal medicine as inducers of apoptosis in cancer treatment. Adv Pharm Bull 2014; 4 Suppl 1: 421-7.

[17]   Sarin YK, Bedi KL, Atal CK. Costus speciosus rhizome as a source of Diosgenin. Current Science 1974; 43: 569-570.

[18]   Pawar VA, Pawar PR. *Costus speciosus*: an important medicinal plant. International Journal of Science and Research 2014; 3: 28-33.

[19]   El-Far AH, Badria FA, Shaheen HM. Possible anticancer mechanisms of some *Costus spe-*

ciosus active ingredients concerning drug discovery. Curr Drug Discov Technol 2016; 13: 123-143.

[20] Khare CP. Indian medicinal plants. India: Springer (India) Private Limited; 2007.

[21] Lijuan W, Kupittayanant P, Chudapongse N, Wray S, Kupittayanant S. The effects of wild ginger, Costus speciosus (Koen Smith) rhizome extract and diosgenin on rat uterine contractions. Reprod Sci 2011; 18: 516-524.

[22] Elkady AI. Anethole inhibits the proliferation of human prostate cancer cells via induction of cell cycle arrest and apoptosis. Anticancer Agents Med Chem 2018; 18: 216-236.

[23] Elkady AI, Hussein RA, El-Assouli SM. Mechanism of action of *nigella sativa* on human colon cancer cells: the suppression of AP-1 and NF-κB transcription factors and the induction of cytoprotective genes. Asian Pac J Cancer Prev 2015; 16: 7943-57.

[24] Repnik U, Turk B. Lysosomal-mitochondrial cross-talk during cell death. Mitochondrion 2010; 10: 662-9.

[25] Zhang L, Jiao M, Li L, Wu D, Wu K, Li X, Zhu G, Dang Q, Wang X, Hsieh JT, He D. Tumorspheres derived from prostate cancer cells possess chemoresistant and cancer stem cell properties. J Cancer Res Clin Oncol 2012; 138: 675-86.

[26] Hamburger AW, Salmon SE. Development of a bioassay for human myeloma colony-forming cells. Proc Natl Acad Sci U S A 1980; 94: 9052-9057.

[27] Guzinska-Ustymowicz K, Pryczynicz A, Kemona A, Czyzewska J. Correlation between proliferation markers: PCNA, Ki-67, MCM2 and anti-apoptotic protein Bcl-2 in colorectal cancer. Anticancer Res 2009; 29: 3049-3052.

[28] Mori S, Chang JT, Andrechek ER, Matsumura N, Baba T, Yao G, Kim JW, Gatza M, Murphy S, Nevins JR. Anchorage-independent cell growth signature identifies tumors with metastatic potential. Oncogene 2009; 28: 2796-2805.

[29] Chaffer CL, Weinberg RA. A perspective on cancer cell metastasis. Science 2011; 331: 1559-1564.

[30] Sellers WR, Fisher D. Apoptosis and cancer drug targeting. J Clin Invest 1999; 104: 1655-1661.

[31] Frankfurt OS, Krishan A. Apoptosis-based drug screening and detection of selective toxicity to cancer cells. Anticancer Drugs 2003; 14: 555-561.

[32] Fulda S, Wick W, Weller M, Debatin KM. Smac agonists sensitize for Apo2L/TRAILor anticancer drug-induced apoptosis and induce regression of malignant gliomas in vivo. Nat Med 2002; 8: 808-815.

[33] Antosiewicz J, Ziolkowski W, Kar S, Powolny AA, Singh SV. Role of reactive oxygen intermedi-ates in cellular responses to dietary cancer chemopreventive agents. Planta Med 2008; 74: 1570-1579.

[34] Česen MH, Pegan K, Spes A, Turk B. Lysosomal pathways to cell death and their therapeutic applications. Exp Cell Res 2012; 318: 1245-51.

[35] Boya P, Kroemer G. Lysosomal membrane permeabilization in cell death. Oncogene 2008; 27: 6434-51.

[36] Dielschneider RF, Henson ES, Gibson SB. Lysosomes as oxidative targets for cancer therapy. Oxid Med Cell Longev 2017; 2017: 3749157.

[37] Kwon KB, Park BH and Ryu DG. Chemotherapy through mitochondrial apoptosis using nutritional supplements and herbs: a brief overview. J Bioenerg Biomembr 2007; 39: 31-34.

[38] Forbes-Hernández TY, Giampieri F, Gasparrini M, Mazzoni L, Quiles JL, Alvarez-Suarez JM, Battino M. The effects of bioactive compounds from plant foods on mitochondrial function: a focus on apoptotic mechanisms. Food Chem Toxicol 2014; 68: 154-82.

[39] Kelly GL, Strasser A. The essential role of evasion from cell death in cancer. Adv Cancer Res 2011; 111: 39-96.

[40] Mackey TJ, Borkowski A, Amin P, Jacobs SC, Kyprianou N. bcl-2/bax ratio as a predictive marker for therapeutic response to radiotherapy in patients with prostate cancer. Urology 1998; 52: 1085-1090.

[41] Van Cruchten S, Van Den Broeck W. **Morpho**logical and biochemical aspects of apoptosis, oncosis and necrosis. Anat Histol Embryol 2002; 31: 214-223.

[42] Yasuhara S, Zhu Y, Matsui T, Tipirneni N, Yasuhara Y, Kaneki M, Rosenzwe A, Martyn JA. Comparison of comet assay, electron microscopy, and flow cytometry for detection of apoptosis. J Histochem Cytochem 2003; 51: 873-85.

[43] Norbury CJ, Zhivotovsky B. DNA damage-induced apoptosis. Oncogene 2004; 23: 2797-2808.

[44] Khan N, Afaq F, Mukhtar H. Apoptosis by dietary factors: the suicide solution for delaying cancer growth. Carcinogenesis 2007; 28: 233-9.

[45] Meeran SM, Katiyar SK. Cell cycle control as a basis for cancer chemoprevention through dietary agents. Front Biosci 2008; 13: 2191-202.

[46] Lu W, Du S, Wang J. Berberine inhibits the proliferation of prostate cancer cells and induces G_0/G_1 or G_2/M phase arrest at different concentrations. Mol Med Rep 2015; 11: 3920-4.

[47] Chen SF, Chang YC, Nieh S, Liu CL, Yang CY, Lin YS. Nonadhesive culture system as a model of rapid sphere formation with cancer stem cell properties. PLoS One 2012; 7: e31864.

[48] Benayoun L, Shaked Y. In vitro enrichment of tumor-initiating cells from human established cell lines. Curr Protoc Stem Cell Biol 2013; Chapter 3: Unit 3.7.

[49] Sheng X, Li Z, Wang DL, Li WB, Luo Z, Chen KH, Cao JJ, Yu C, Liu WJ. Isolation and enrichment of PC-3 prostate cancer stem-like cells using MACS and serum-free medium. Oncol Lett 2013; 5: 787-792.

[50] Patrawala L, Calhoun T, Schneider-Broussard R, Zhou J, Claypool K, Tang DG. Side population is enriched in tumorigenic, stem-like cancer cells, whereas ABCG2+ and ABCG2- cancer cells are similarly tumorigenic. Cancer Res 2005; 65: 6207-6219.

[51] Palapattu GS, Wu C, Silvers CR, Martin HB, Williams K, Salamone L, Bushnell T, Huang LS, Yang Q, Huang J. Selective expression of CD44, a putative prostate cancer stem cell marker, in neuroendocrine tumor cells of human prostate cancer. Prostate 2009; 69: 787-798.

[52] Patrawala L, Calhoun T, Schneider-Broussard R, Li H, Bhatia B, Tang S, Reilly JG, Chandra D, Zhou J, Claypool K, Coghlan L, Tang DG. Highly purified CD44+ prostate cancer cells from xenograft human tumors are enriched in tumorigenic and metastatic progenitor cells. Oncogene 2006; 25: 1696-1708.

[53] Polyak K, Hahn WC. Roots and stems: stem cells in cancer. Nat Med 2006; 12: 296-300.

[54] Scarpa ES, Ninfali P. Phytochemicals as innovative therapeutic tools against cancer stem cells. Int J Mol Sci 2015; 16: 15727-42.

[55] Pistollato F, Giampieri F, Battino M. The use of plant-derived bioactive compounds to target cancer stem cells and modulate tumor microenvironment. Food Chem Toxicol 2015; 75: 58-70.

[56] Shruti Srivastava, Pradeep Singh, Garima Mishra1, K. K. Jha1, R. L. Khosa. *Costus speciosus* (Keukand): a review. Der Pharmacia Sinica 2011; 2: 118-128.

[57] Eliza J, Daisy P, Ignacimuthu S, Duraipandiyan V. Normo-glycemic and hypolipidemic effect of costunolide isolated from *Costus speciosus* (Koen ex. Retz.) Sm. in streptozotocin-induced diabetic rats. Chem Biol Interact 2009; 179: 329-34.

[58] Hsu JL, Pan SL, Ho YF, Hwang TL, Kung FL, Guh JH. Costunolide induces apoptosis through nuclear calcium^{2+} overload and DNA damage response in human prostate cancer. J Urol 2011; 185: 1967-74.

[59] Lin X, Peng Z and Su C. Potential anti-cancer activities and mechanisms of costunolide and dehydrocostuslactone. Int J Mol Sci 2015; 16: 10888-10906.

[60] Peng Z, Wang Y, Fan J, Lin X, Liu C, Xu Y, Ji W, Yan C, Su C. Costunolide and dehydrocostuslactone combination treatment inhibit breast cancer by inducing cell cycle arrest and apoptosis through c-Myc/p53 and AKT/14-3-3 pathway. Sci Rep 2017; 7: 41254.

[61] Zhuge W, Chen R, Vladimir K, Dong X, Zia K, Sun X, Dai X, Bao M, Shen X, Liang G. Costunolide specifically binds and inhibits thioredoxin reductase-1 to induce apoptosis in colon cancer. Cancer Lett 2018; 412: 46-58.

[62] Eliza J, Daisy P, Ignacimuthu S. Antioxidant activity of costunolide and eremanthin isolated from Costus speciosus (Koen ex. Retz) Sm. Chem Biol Interact 2010; 188: 467-472.